Analysis and visualization of multiply oriented lattice structures by a two-dimensional continuous wavelet transform

H. M. Singer*
Institute of Low Temperature Science ILTS, Hokkaido University, 060-0819 Sapporo, Japan

I. Singer†
Institute for Electronic Science RIES, Hokkaido University, 060-0812 Sapporo, Japan

(Received 4 April 2006; revised manuscript received 10 June 2006; published 6 September 2006)

The phase-field-crystal model [K. R. Elder and M. Grant, Phys. Rev. E **70**, 051605 (2004)] produces multigrain structures on atomistic length scale but on diffusive time scales. Since individual atoms are resolved but are treated identically it is difficult to distinguish the exact position of grain boundaries and defects within grains. In order to analyze and visualize the whole grains a two-dimensional wavelet transform has been developed, which is capable of extracting grain boundaries and the lattice orientation of a grain relative to a laboratory frame of reference. This transformation makes it possible not only to easily visualize the multigrain structure, but also to perform exact measurements on low- and high-angle boundaries, grain size distributions and boundary-angle distributions, which can then be compared to experimental data. The presented wavelet transform can also be applied to results of other atomistic simulations, e.g., molecular dynamics or granular materials.

DOI: 10.1103/PhysRevE.74.031103 PACS number(s): 05.70.Ln, 95.75.Mn, 64.60.Cn, 64.60.My

I. INTRODUCTION

A recently developed phase-field-crystal (PFC) model [1] describes nonequilibrium processes in materials such as solidification, grain growth, epitaxial growth, and material hardness. The PFC model takes into account elastic properties of materials and, for the first time in phase-field modelling, the actual lattice structure. The order parameter describing the density field on the nanoscale is constant in the liquid phase and periodic in the solid phase. Since the model works on atomistic length scales, simulating interesting dynamics on the mesoscale requires extremely large computational domains. A renormalization group approach was applied in Ref. [2] to parametrize the density field in terms of a uniform phase and an amplitude. This approach allows to solve the PFC equation on the mesocale using adaptive meshes and then to reconstruct the density field on the nanoscale.

The renormalization group approach is very efficient numerically and provides the lattice orientation information, however this information can only be retrieved if the PFC equation is renormalized and solved in terms of the phase and amplitude from the very beginning.

As opposite to the conventional phase-field models for grain growth [3,4], the PFC method does not have a mechanism to distinguish between areas with different lattice orientations, i.e., grains. When the PFC equation is solved directly, i.e., for the density field, as has been proposed in the original PFC paper [1], analysis and visualization of a grain structure are difficult even in relatively small domains containing only several thousand atoms.

The equation of motion for the time averaged evolution of the density field ρ is derived from a dimensionless free energy functional

$$\mathcal{F} = \int d\mathbf{r}\left(\frac{\rho}{2}[r + (1+\nabla^2)^2]\rho + \frac{\rho^4}{4}\right), \tag{1}$$

where $G(\nabla^2)=(1+\nabla^2)^2$ is the functional form of a fit to the first order peak of an experimental structure factor and r is the dimensionless undercooling. The resulting time-dependent density field equation is derived from the functional derivative by the Cahn-Hilliard formalism,

$$\frac{\partial \rho}{\partial t} = \nabla^2[r + (1+\nabla^2)^2\rho + \rho^3]. \tag{2}$$

The equation contains a sixth order spatial derivative and therefore requires very small time steps if solved with an explicit finite difference scheme.

In the case of classical molecular dynamics simulations every single particle, its position and velocity at every time step is known. In the simplest case of monoatomistic simulations the next time step is calculated based on the current position and velocity and the interaction forces with (in principle) all other atoms in the simulation domain based on the classical Newton equations of motion [5]

$$m\frac{d^2\mathbf{r}_i(t)}{dt^2} = \mathbf{f}_i = \sum_{j=1, j\neq i}^{N_{\mathrm{at}}} \mathbf{f}_{\mathbf{ij}}, \tag{3}$$

where $\mathbf{r_i}$ is the position of the ith atom and $\mathbf{f_{ij}}=-\boldsymbol{\nabla} U(r) = -\boldsymbol{\nabla} U(\|\mathbf{r_i}-\mathbf{r_j}\|)$ is the pairwise force calculated from a potential function U.

In this kind of simulation solidification of small grains or clusters can be produced. A convenient measure of atomistic defects in the crystalline structure is the particle potential energy

*Electronic address: hsinger@solid.phys.ethz.ch
†Electronic address: irina@mech.kth.se

$$E_{U,i} = \frac{4}{N_{\text{at}}} \sum_{j=1}^{N_{\text{at}}} U_{ij}, \tag{4}$$

where $U_{ij} = U(\|\mathbf{r_i} - \mathbf{r_j}\|)$ is the pairwise potential energy interaction between the atom i and another atom j. Since the potential for monoatomistic simulations is only a function of the distance between the atoms, it is rotational invariant. Therefore a solidified structure such as a set of grains has the same potential energy everywhere when the crystal lattice is regular independent of the orientation. The potential energy reveals only differences on the grain boundaries and at lattice defects. In order to find the grain orientation additional measurements must be performed. As will be shown the technique developed to visualize and analyze the continuum PFC simulations proves also to be useful as an alternative and additional evaluation tool for molecular dynamics simulations.

Wavelets are mathematical functions with a compact support, which analyze different frequency components with a resolution matched to their scale. An advantage over conventional Fourier methods is that they give a better spatial resolution where a frequency component is to be found in comparison to windowed Fourier transforms or Gabor transforms. Wavelets are used in a variety of fields reaching from mathematics and quantum physics to electrical engineering and seismic geology (e.g., Refs. [6–9]).

In order to visualize their results Elder and Grant [1] used a smoothing density field method, which when applied to the results of the PFC calculations revealed grain boundaries and lattice defects as local energy density. This approach, however does not provide any information about the grain orientation, since the smoothing is rotational invariant. In order to find the lattice orientation two trivial approaches can be imagined: (1) find for every atom its neighboring atoms and calculate the angle with respect to a laboratory frame. This approach is in principal straightforward, however it is soon discovered that (i) it is not so easy to detect the positions of the atoms since their maximum might not coincide with the raster of the computational domain and (ii) especially in the regions with lattice defects or grain boundaries it is not clear at all how to define the nearest neighbors, and (iii) due to the above reasons even on a regular lattice calculating the angle is error-prone. (2) The second approach is slightly more elegant: by selecting an atom and a neighborhood of 2^n ($n=5-7$) grid points a fast two-dimensional (2D) Fourier transform is applied on this domain. On a regular lattice the orientation of the lattice is highlighted as a spike in the Fourier spectrum. The procedure becomes problematic however in the case of multiple lattices or lattice defects which destroy the spikes and add noise to the spectrum, which makes a grain orientation detection for this point at least difficult if not impossible. Because of the above-mentioned reasons a straightforward approach to a visualization of grain boundaries and simultaneously grain orientations is not possible. Therefore a special approach combining the smoothing for constant lattice structures while preserving their grain orientation, without having to deal with the above described disadvantages, is desirable. In this paper we present a developed

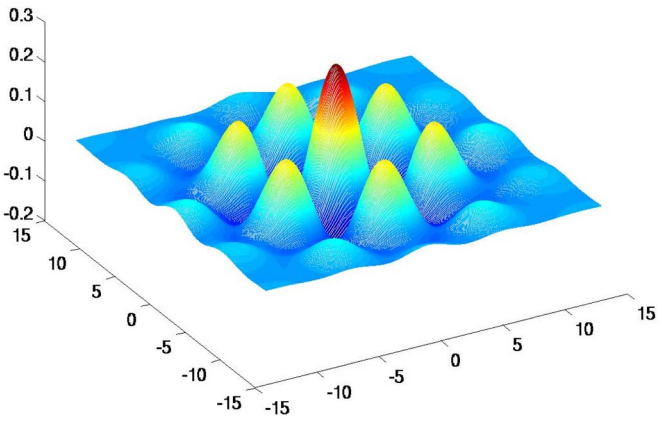

FIG. 1. (Color online) The continuous 2D wavelet. The shape of the wavelet is adjusted to the hexagonal lattice structure produced by the PFC method.

2D continuous wavelet transform, which allows one to visualize and analyze results of large-scale atomistic simulations especially produced by the original PFC method proposed in Ref. [1] for a big domain of tens of thousands to millions of atoms.

II. 2D CONTINUOUS WAVELET TRANSFORM

The PFC model describes the temporal evolution of a density field $\rho(x,y)$. The crystal phase is given as a constant value in the liquid and an oscillatory function in the solid. In 2D the oscillatory function describes a hexagonally closed packed pattern. A fully solidified crystal without defects can be described as the superposition of three planar waves

$$\rho[\vec{x} = (x,y)] = A_0 + a[\cos(\vec{k}_1 \cdot \vec{x}) + \cos(\vec{k}_2 \cdot \vec{x}) + \cos(\vec{k}_3 \cdot \vec{x})], \tag{5}$$

where A_0 is an assumed constant background and a is the amplitude of the hills. The vectors $\vec{k}_1$, $\vec{k}_2$, and $\vec{k}_3$ define the three base vectors of the hexagonal lattice. The vectors are coupled through $\vec{k}_2 = R_{\pi/3}(\vec{k}_1)$, $\vec{k}_3 = R_{\pi/3}[R_{\pi/3}(\vec{k}_1)]$, where $R_\theta(\vec{v})$ is the 2D rotation of the vector v by an angle θ.

In order to find the different lattice orientations and thus distinguish the different grains we use the wavelet formalism and introduce a mother wavelet. Since the lattice spacing and thus the frequency is the same in all grains we fix our wavelet scale on only one particular scale—the one of the lattice frequency. Opposite to the more traditional mother wavelets such as Morlet, Gaussian, Mexican hat or others [6] we introduce a continuous wavelet, which is two dimensional and matches the requirements of the lattice structure. The wavelet is shown in Fig. 1 and is defined as

$$w_{s_0} = \frac{1}{\sqrt{\pi\sigma}} e^{-(x^2+y^2)/2\sigma} (\cos(\vec{k}_{s_0} \cdot \vec{x}) + \cos[R_{\pi/3}(\vec{k}_{s_0}) \cdot \vec{x}] + \cos\{R_{\pi/3}[R_{\pi/3}(\vec{k}_{s_0})] \cdot \vec{x}\}), \tag{6}$$

where the parameter s_0 and subsequently k_{s_0} define the base scale in which we are interested and σ defines the Gaussian

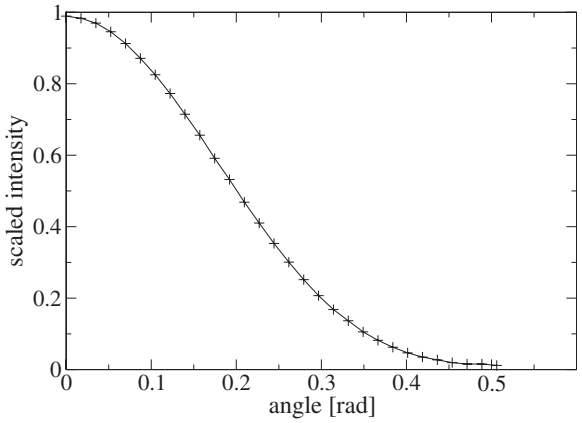

FIG. 2. The intensity profile depends nonlinearly on the lattice mismatch angle. The angle is found first by calculating the average intensity of the grain and then the use of this plot as a look-up table.

support of the wavelet. Applying this wavelet on the domain $\rho(x,y)$ transforms the lattice structures into a similar pattern where the amplitude a is now dependent on the orientation. Therefore the average intensity of the grain is a function of the orientation. In order to transform the oscillation into a constant value we apply a Gaussian transformation

$$G(x,y) = \frac{1}{\sqrt{\pi\sigma_2}} e^{-(x^2+y^2)/2\sigma_2}, \tag{7}$$

where σ_2 defines the smoothing range of the Gaussian filter.

Combining Eqs. (6) and (7) we find $\tilde{\rho}(x,y) = [(\rho * w_{s_0}) * G](x,y)$ where $*$ defines the convolution operator. More explicitly $\tilde{\rho}(x,y)$ is written as

$$\tilde{\rho}(x,y) = \int_{-\infty}^{\infty}\int_{-\infty}^{\infty}\left(\int_{-\infty}^{\infty}\int_{-\infty}^{\infty}\rho(t,u)w_{s_0}(t-v,t-w)dtdu\right) \times G(v-x,w-y)dvdw. \tag{8}$$

The intensity $\tilde{\rho}(x,y)$ is a function of the lattice mismatch between the grain orientation at the position (x,y) and the laboratory frame of reference. The intensity depends nonlinearly on this mismatch angle. In Fig. 2 the transformation is plotted. In order to find the angle the average intensity of the grain is calculated and then transformed back with help of the transfer look-up table of Fig. 2.

For the implementation we have introduced two 2D filter templates t_1 and t_2 with the size $N=41$, which define two $N\times N$ finite supports for the transformations given by Eqs. (6) and (7). This size is suitable to accommodate several atoms for the chosen set of simulation parameters, which led to an average distance of $d_{\text{avg}}=9$ grid points between the atoms in the solidified structure, thus $k_{s_0}=2\pi/d_{\text{avg}}$. The templates were filled with values according to Eqs. (6) and (7) with $\sigma=0.3N$ and $\sigma_2=0.5N$ with the origin taken in the center of the templates. Subsequently the simulation data was convolved with t_1,

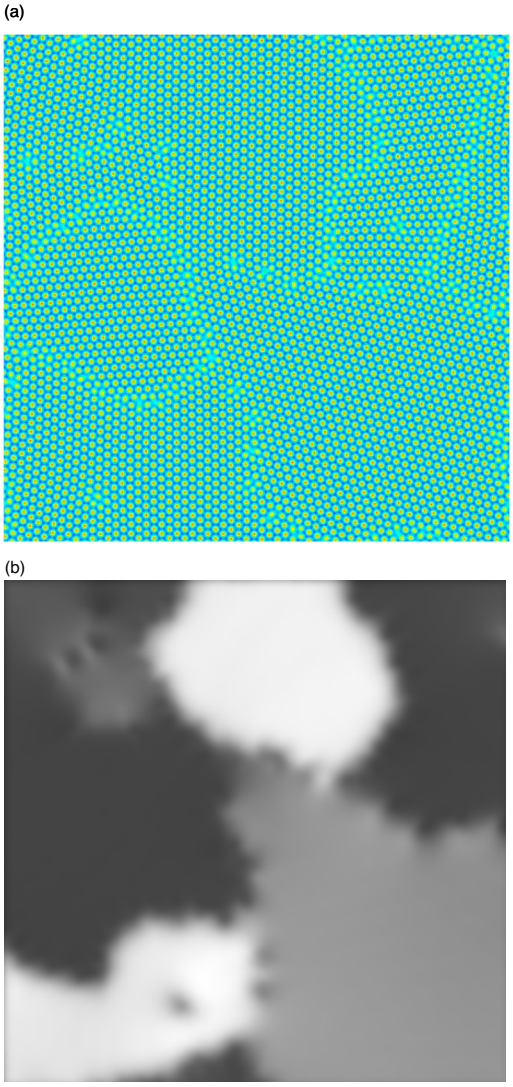

FIG. 3. (Color online) (a) The density field calculated by the PFC model in a 512×512 box. (b) The corresponding grain structure obtained by the 2D wavelet transformation. The different grains contain a constant value depending on their orientation. The value changes only at the grain boundary.

$$\rho_{1,i,j} = \sum_{l=-N/2}^{N/2}\sum_{m=-N/2}^{N/2} t_{1,N/2+m,N/2+l}\rho_{i+m,j+l}. \tag{9}$$

And then $\tilde{\rho}$ was obtained by convolving ρ_1 with t_2 in the same way.

III. RESULTS

First, we demonstrate the results of the PFC simulations and subsequent wavelet transformation in a computational domain of size 512×512 grid nodes, which contains approximately 4000 atoms. The size of the domain is in purpose taken very small in order to demonstrate the lattice structure of the grains. The parameters used for the PFC simulations are $r=-0.25$ and $\bar{\rho}=-0.28$. Figure 3(a) shows the

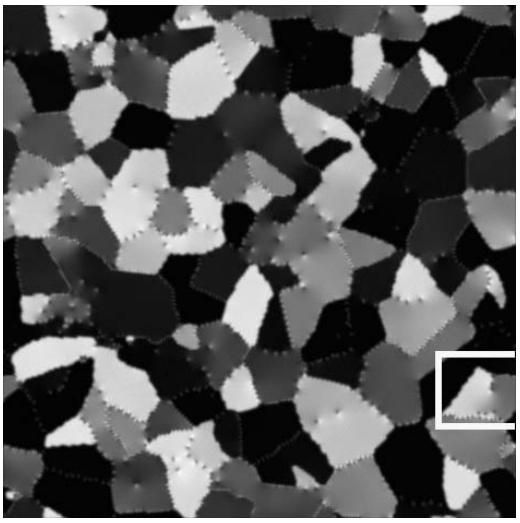

FIG. 4. The grain structure obtained by the 2D wavelet transformation of the density field calculated by the PFC model in a 4096×4096 box. The intensity corresponds to the grain orientation. The white box shows a grain where a defect causes the grain's orientation to change.

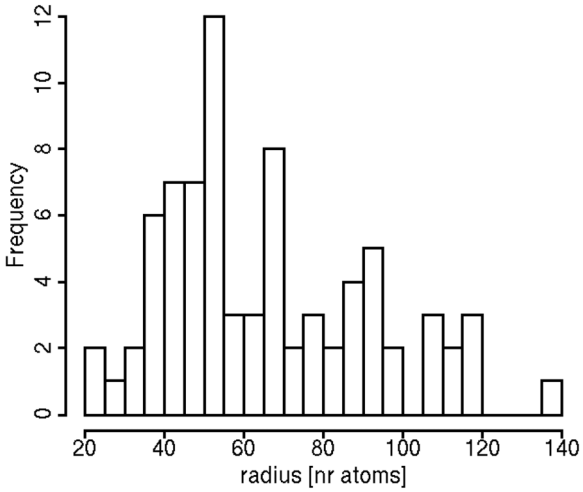

FIG. 5. Histogram of the grain size distribution of Fig. 4, where on the x axis "nr" denotes the number of atoms.

density field obtained by the PFC simulations. One observes a well-defined lattice structure within each grain. In this small domain it is also possible to extract visually the position of the grain boundaries and missorientation between the grains. A corresponding grain structure produced by the wavelet transformation is shown in Fig. 3(b). Every grain can easily be identified by its gray scale intensity dependent on the lattice orientation, where white depicts a maximal alignment and black a maximal mismatch.

Next the PFC simulations were performed in the domain of 4096×4096 grid nodes, which contains approximately 262 100 atoms. Obviously, no information can be extracted visually from the density field even on a large computer screen. Figure 4 demonstrates the result of the wavelet transformation applied to the density field. The location of the grains, grain boundaries and lattice defects are clearly pronounced. The transformation also indicates very accurately the lattice defects within a single grain. Examples can be found in Fig. 4 in several grains. It is interesting to note that a lattice defect can influence the orientation of the whole grain. In the white box on the right-hand side of Fig. 4 there is a grain, which changes its orientation gradually due to a defect.

The wavelet transform also allows to easily analyze the grain formation produced by the PFC method. In particular, it is possible to evaluate automatically the number of atoms within each grain. A histogram showing the distribution of grain sizes is given in Fig. 5. The average grain radius is about 55 atoms for the grain structure in Fig. 4. In the analysis, the grains, whose lattice orientation varied more than 5% due to presence of defects, were classified as two grains. This technique can be applied for studying grain coarsening, which is an important problem in materials science (e.g., Refs. [10–12]). Also, the wavelet transformation automatically reveals low- and high-angle grains when the two neighboring grains have similar and different gray levels, respectively.

Elder and Grant [1] have demonstrated that the PFC method reproduces correctly the Read-Shockley grain boundary energy for small missorientations. In order to evaluate the Read-Shockley energy it is essential to know the distribution of dislocations at the grain boundary. While it is straightforward to do it for planar grain boundaries using geometrical arguments, defining positions of the dislocations on curved grain boundaries can be difficult. The wavelet transform allows to extract information on the dislocation distribution for curved boundaries for small enough missorientations angles ($<12-15$ degrees). As an example, Fig. 6 shows an arbitrarily shaped grain embedded in a large grain whose orientation differs by 8 degrees as a density field (a) and the corresponding wavelet transform (b). Obviously, the wavelet transform provides a clear picture on the number of dislocations and their positions. They can be found automatically by selecting the extrema of the white regions.

The study of atomistic grain boundaries in molecular dynamics has recently gained more attention. On the one hand, it is possible to calculate the interfacial stiffness from the atomistic fluctuations of the solid-liquid interface [13] and therefore the strength of the anisotropy of surface free energy. On the other hand, the atomistic behavior of solidified grains and their evolutions is subject of research for short time scales accessible in MD simulations as well [14]. In Fig. 7(a) a very simple constellation of two misoriented grains and their grain boundary is plotted. The atoms at the grain boundary possess a higher potential energy than the atoms in the regular crystal lattice of the grains. The potential energy is a convenient means to find the grain boundary between grains, however its value is identical in any grain that has an ordered lattice structure. The presented wavelet transform can be used to extract this information easily by rasterizing the domain and substituting the positions of the atoms with a short-range continuous function

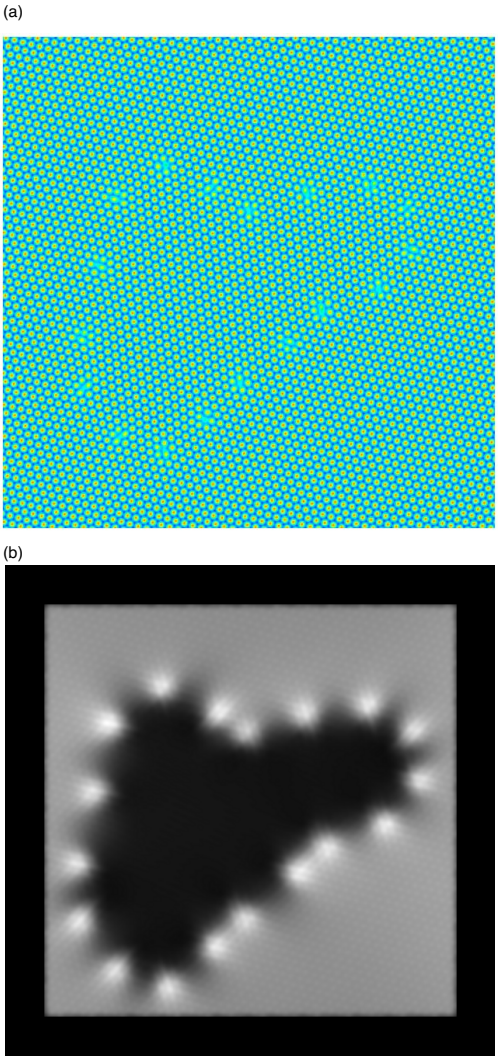

FIG. 6. (Color online) An arbitrarily shaped grain embedded in a larger grain shown as (a) density field, (b) corresponding wavelet transform. The misorientation between the two grains is 8 degrees. The wavelet transform reveals clearly the location of dislocations at the grain boundary as white maxima. The simulation was performed in a 512×512 box.

$$v_{i+l,j+m}(k) = \sum_{n=1}^{N_{\text{at}}} B_a \left[\cos\left(\frac{i(k)+l}{a} \pi \right) + \cos\left(\frac{j(k)+m}{a} \pi \right) \right] \tag{10}$$

with $-a \leqslant l \leqslant a$, $-a \leqslant m \leqslant a$ where v_{ij} is the value at the raster position (i,j) calculated for the atom k $[i(k),j(k)]$, and $B_a(d)=d$ for $d \leqslant a$ and otherwise zero. The principle is simply to replace the position of the atoms by a cosine-shaped bump around every atom in the raster. This leads to a similar raster image as Fig. 3(a). The according wavelet transformation is shown in Fig. 7(b). While for this example the transformation seems overly elaborate it can easily be imagined that large scale MD simulations with a multitude of grains would benefit from this transformation in order to extract the orientation of the grains as an alternative analysis method.

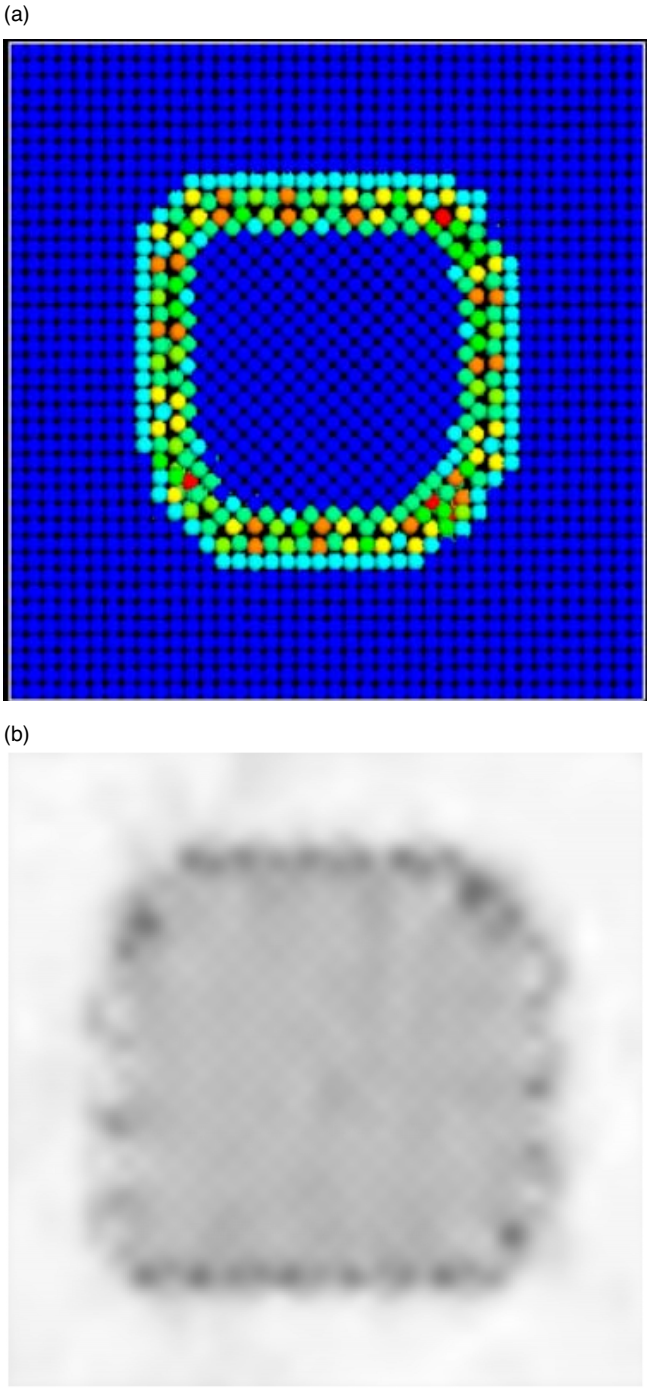

FIG. 7. (Color online) (a) Two grains in a molecular dynamics simulation in order to investigate the atomistic behavior at the grain boundary (courtesy of T. Uehara, Nagoya University, Japan). The atoms near the grain boundary have a higher potential energy than the ones far away from the grain boundary. Their potential energy is identical in both grains independent on orientation. (b) Application of the 2D wavelet transform, which in this case extracts the orientation of the grains in the MD simulations.

IV. GENERALIZATION

The presented wavelet can easily be extended and generalized (i) to analyze three-dimensional data and (ii) to include different lattice structures or different sorts of atoms

e.g., for binary alloy systems). Equation (6) was developed with a 2D fcc or hexagonal lattice in mind. In a more general way the equation can be rewritten as

$$w_{s_0} = \frac{1}{\sqrt{\pi\sigma}} \exp^{-\sum_{i=1}^{d} x_i^2/2\sigma} V_{s_0}(x_1, \ldots, x_d), \tag{11}$$

where d is the dimension and V_{s_0} is a representative description of the lattice defined in the support region of the Gaussian, which is relevant at the scale s_0. Since the goal is not to analyze the structure at different scales V_{s_0} can be chosen to be the repeated unit cell over the support, where the unit cell may contain different sorts of atoms.

V. CONCLUSION

We have presented a 2D continuous wavelet transform, which allows the analysis and visualization of large scale atomistic simulations. Applied to the density field produced by the PFC model, the wavelet transform extracts the grains and their orientation with respect to a laboratory frame of reference. This simplifies the task of determining grain sizes and grain boundary angles. Applied to rasterized MD data the transform serves as an alternative tool, additional to the potential energy, to analyze and visualize solidified grains.

Additional to its originally intended use for the large domains of the PFC model the presented method has other potential applications, for example, in high resolution electron microscopy, where grain boundaries are still mostly evaluated manually, flux lines of superconductors or images of experiments with hard spheres or simulations thereof (granular media). We believe that the presented method might be applied also in other physical phenomena where atomistic or spherical particles are to be analyzed in a larger scale.

ACKNOWLEDGMENTS

One of the authors (H.M.S.) is supported by the Japanese Society for the Promotion of Science (JSPS). One of the authors (I.S.) is funded by the NXO project (project leader Dr. Kinoshita, CRIEPI), Japan. The authors thank Professor Kobayashi, Hiroshima University, Japan for providing an efficient solver for the PFC equation.

[1] K. R. Elder and M. Grant, Phys. Rev. E **70**, 051605 (2004).
[2] N. Goldenfeld, B. P. Athreya, and J. A. Dantzig, Phys. Rev. E **72**, 020601(R) (2005).
[3] J. A. Warren, W. C. Carter, and R. Kobayashi, Physica A **261**, 159 (1998).
[4] J. Z. Zhu, T. Wang, A. J. Ardell, S. H. Zhou, Z. K. Liu, and L. Q. Chen, Acta Mater. **52**, 2837 (2004).
[5] D. C. Rapaport, *The Art of Molecular Dynamics Simulation* (Cambridge University Press, Cambridge, 2004).
[6] D. F. Walnut, *An Introduction to Wavelet Analysis* (Birkhäuser, Boston, 2004).
[7] C. C. Chaston, T. D. Phan, J. W. Bonnell, F. S. Mozer, M. Acuna, M. L. Goldstein, A. Balogh, M. Andre, H. Reme, and A. Fazakerley, Phys. Rev. Lett. **95**, 065002 (2005).
[8] P. Manimaran, P. K. Panigrahi, and J. C. Parikh, Phys. Rev. E **72**, 046120 (2005).
[9] P. C. Whitford and G. D. J. Phillies, Phys. Rev. E **72**, 021203 (2005).
[10] A. K. Koul and F. B. Pickering, Acta Metall. **30**, 1303 (1982).
[11] K. He and T. N. Baker, Mater. Sci. Eng., A **256**, 111 (1998).
[12] S.-H. Hong and D. N. Lee, Mater. Sci. Eng., A **357**, 75 (2003).
[13] J. J. Hoyt, M. Asta, and A. Karma, Phys. Rev. Lett. **86**, 5530 (2001).
[14] T. Uehara (private communication).